Dihydridoamine and Hydridoamido Complexes of Ruthenium(II) with a Tetradentate P−N−N−P Donor Ligand

Tianshu Li, Raphaël Churlaud, Alan J. Lough, Kamaluddin Abdur-Rashid,† and Robert H. Morris*

Department of Chemistry, University of Toronto, 80 St. George Street, Toronto, Ontario M5S 3H6, Canada

Received June 14, 2004

The new diphosphinediimine ligand $PPh_2C_6H_4CH{=}NCMe_2CMe_2N{=}CHC_6H_4PPh_2$ {$tmeP_2N_2$} is prepared by reacting $NH_2CMe_2CMe_2NH_2$ with 2 equiv of $PPh_2(C_6H_4$-2-CHO). The diamine derivative $PPh_2C_6H_4CH_2NHCMe_2CMe_2NHCH_2C_6H_4PPh_2$ {$tmeP_2(NH)_2$} is prepared by reducing $tmeP_2N_2$ with $LiAlH_4$. The reaction of $RuHCl(PPh_3)_3$ with $tmeP_2N_2$ in THF produces the complex *trans*-RuHCl{$tmeP_2N_2$}, while a similar reaction of $RuHCl(PPh_3)_3$ with $tmeP_2(NH)_2$ gives the complex *trans*-RuHCl{$tmeP_2(NH)_2$}, as a mixture of two isomers. The isomer with two N−H bonds *syn* to the Ru−H bond is converted on heating to an isomer thought to have one N−H *syn* to the Ru−H. The reaction of the two isomers with KO^{t}Bu under Ar in toluene produces the novel hydridoamido complex RuH{$tmeP_2NNH$}, where the ligand is deprotonated at one nitrogen. Reaction of this amido complex with H_2 gives exclusively the dihydridoamine complex *trans*-Ru(H)$_2${$tmeP_2(NH)_2$}. The complexes have been characterized by X-ray crystallography, NMR, IR, elemental analysis, and a deuterium exchange study. Complex RuH{$tmeP_2NNH$}, or a combination of RuHCl{$tmeP_2(NH)_2$} and KO^{t}Bu, slowly catalyzes the hydrogenation of acetophenone (6 atm H_2, 20 °C, benzene or 2-propanol). The catalytic cycle is thought to be similar to that for the ketone hydrogenation precatalyst *trans*-RuHCl{(S,S)-$cyP_2(NH)_2$)}. However in the present work both of the proposed catalysts *trans*-RuH_2{$tmeP_2(NH)_2$} and RuH{$tmeP_2NNH$} have been completely characterized. The $tmeP_2(NH)_2$ system, with hindering methyl groups, is less active than the $cyP_2(NH)_2$ system with a *trans*-1,2-substituted cyclohexyl backbone. The variable configuration of the amine nitrogens that is observed for the $tmeP_2(NH)_2$ complexes might also occur in the $cyP_2(NH)_2$ systems and could explain the inconsistent selectivity of such catalysts. The diimine complex RuHCl{$tmeP_2N_2$} reacts with KO^{t}Bu under H_2 to produce the dihydridodiamine complex *trans*-Ru(H)$_2${$tmeP_2(NH)_2$}, the catalyst for the hydrogenation of acetophenone.

Introduction

Over the past several years, a variety of tetradentate $Ph_2P-N-Z-N-PPh_2$ ligands with different amine backbone linkers Z (where PPh_2 is a diphenylphosphino group and N is an amine or an imine donor) have been prepared by Gao et al. (Chart 1).[1−4] These were used to make ruthenium and rhodium precatalysts for the asymmetric hydrogenation of ketones.[1−4]

These tetradentate ligands possess two "soft" phosphorus atoms and two "hard" nitrogen atoms that restrict the coordination geometry around ruthenium, usually to the *trans* isomer.[2] However *cis*-*β*-dichloro complexes have also been prepared and other isomers are also conceivable. The five-coordinate cationic complexes of the type $[RuCl(PPh_2-NH-NH-PPh_2)]^+$, prepared by chloride abstraction from $[RuCl_2(PPh_2-NH-NH-PPh_2)]$, catalyze the epoxidation of olefins with hydrogen peroxide[5] or air[6] as oxidant and the cyclopropanation of olefins.[7,8] The ruthenium hydridochloro complexes *trans*-$RuHCl(PPh_2-NH-NH-PPh_2)$ have proven to be active precatalysts for transfer hydrogenation and H_2-hydrogenation[9] of ketones to alcohols. The relatively rigid, chiral, tetradentate ligand complexes lead to enantioselective transfer hydrogenation reactions,[3] but less selective H_2-hydrogenation.[9] The kinetics and mechanism of hydrogenation of acetophenone to 1-phenylethanol catalyzed by *trans*-RuHCl{(*S,S*)-$cyP_2(NH)_2$} (**1**) and alkoxide have recently been described.[9] The proposed mechanism is shown in Scheme 1. The reaction of precatalyst **1** with the base is thought to

* To whom correspondence should be addressed. E-mail: rmorris@chem.utoronto.ca.
† Present address: Kanata Chemical Technologies, 2240 Speakman Dr., Sheridan Science and Technology Park, Mississauga, Ontario, L5K 1A9, Canada.

(1) Gao, J.-X.; Ikariya, T.; Noyori, R. *Organometallics* **1996**, *15*, 1087−1089.
(2) Gao, J.-X.; Wan, H.-L.; Wong, W.-K.; Tse, M.-C.; Wong, W.-T. *Polyhedron* **1996**, *15*, 1241−1251.
(3) Gao, J.-X.; Zhang, H.; Yi, X.-D.; Xu, P.-P.; Tang, C.-L.; Wan, H.-L.; Tsai, K.-R.; Ikariya, T. *Chirality* **2000**, *12*, 383−388.
(4) Gao, J.-X.; Xu, P.-P.; Yi, X.-D.; Yang, C.-B.; Zhang, H.; Cheng, S.-H.; Wan, H.-L.; Tsai, K.-R.; Ikariya, T. *J. Mol. Catal. A* **1999**, *147*, 105−111.
(5) Stoop, R. M.; Bachmann, S.; Valentini, M.; Mezzetti, A. *Organometallics* **2000**, *19*, 4117−4126.
(6) Wong, W.-K.; Chen, X.-P.; Chik, T.-W.; Wong, W.-Y.; Guo, J.-P.; Lee, F.-W. *Eur. J. Inorg. Chem.* **2003**, 3539−3546.
(7) Bachmann, S.; Furler, M.; Mezzetti, A. *Organometallics* **2001**, *20*, 2102−2108.
(8) Bonaccorsi, C.; Bachmann, S.; Mezzetti, A. *Tetrahedron Asymmetry* **2003**, *14*, 845−854.
(9) Rautenstrauch, V.; Hoang-Cong, X.; Churlaud, R.; Abdur-Rashid, K.; Morris, R. H. *Chem. Eur. J.* **2003**, *9*, 4954−4967.

10.1021/om049565k CCC: $27.50
Publication on Web 11/20/2004

Chart 1

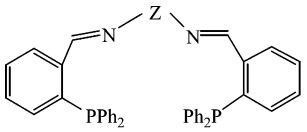

ZP_2N_2

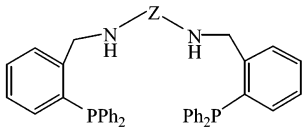

$ZP_2(NH)_2$

Ref.	Z	diimine	diamine
2, 3, 5	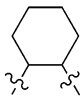	cyP_2N_2	$cyP_2(NH)_2$
2, 5	$-CH_2CH_2-$	enP_2N_2	$enP_2(NH)_2$
1, 4	$-CH_2CH(Me)-$	MeP_2N_2	$MeP_2(NH)_2$
this work	$-CMe_2CMe_2-$	$tmeP_2N_2$	$tmeP_2(NH)_2$

Scheme 1

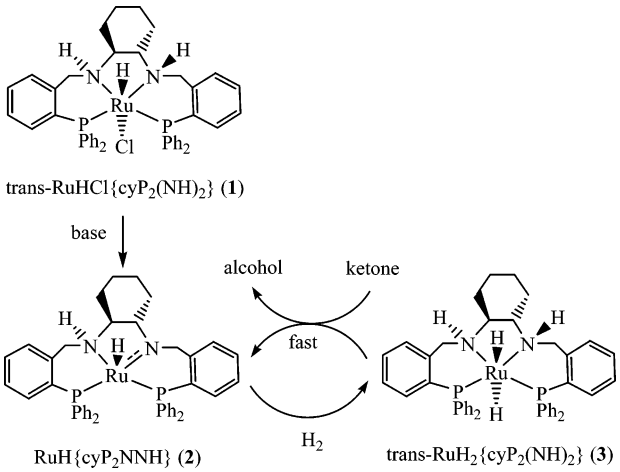

produce a reactive hydridoamido complex, RuH($PPh_2C_6H_4CH_2NC_6H_{10}NHCH_2C_6H_4PPh_2$), abbreviated as RuH{$cyP_2NNH$} (**2**), that could not be isolated. Dihydrogen adds across the ruthenium−amido bond in the turnover limiting step to give the dihydridoamine complex *trans*-$RuH_2\{cyP_2(NH)_2\}$ (**3**). Experiments proved that *trans* and *cis* dihydrides can be generated in solution.[9] The hydride complex in the catalytic cycle is thought to be *trans* by analogy with the ketone hydrogenation catalyst *trans*-RuH_2(binap)(tmen), tmen = $NH_2CMe_2CMe_2NH_2$, prepared from RuH(binap)($NHCMe_2CMe_2NH_2$) with H_2. The use of the methylated diamine tmen, which lacks hydrogen atoms alpha to the amine groups, allowed the isolation and complete characterization of these hydrogenation catalysts.[10] The corresponding amido and dihydride complexes prepared with the new tetradentate ligand $PPh_2C_6H_4CH_2NHCMe_2CMe_2NHCH_2C_6H_4PPh_2$ {$tmeP_2(NH)_2$} have now been isolated and fully characterized.

Experimental Section

General Procedures. All preparations and manipulations were carried out under hydrogen, nitrogen, or argon atmospheres with the use of standard Schlenk, vacuum line, and glovebox techniques in dry, oxygen-free solvents. Tetrahydrofuran (THF), diethyl ether (Et_2O), and hexanes were dried and distilled from sodium benzophenone ketyl. Deuterated solvents were degassed and dried over activated molecular sieves. Potassium *tert*-butoxide and 2-(diphenylphosphino)benzaldehyde were supplied by the Aldrich Chemical Co. The diamine $NH_2CMe_2CMe_2NH_2$[11] and the complex $RuHCl(PPh_3)_3$[12] were prepared by the literature methods. NMR spectra were recorded on a Varian Unity-500 (500 MHz for ^1H), a Varian Unity-400 (400 MHz for ^1H), or a Varian Gemini 300 MHz spectrometer (300 MHz for ^1H and 121.5 for ^{31}P). All ^{31}P chemical shifts were measured relative to 85% H_3PO_4 as an external reference. ^1H chemical shifts were measured relative to partially deuterated solvent peaks but are reported relative to tetramethylsilane. All infrared spectra were obtained on a Nicolet 550 Magna-IR spectrometer. Microanalyses and mass spectroscopy were performed at the University of Toronto. Hydrogenation reactions were done at constant pressures of H_2 using a 50 mL Parr hydrogenation reactor. The Parr hydrogenation reactor was flushed several times with hydrogen gas at the preset pressure prior to adding the reaction mixture or its components. Aliquots of the reaction mixture were quickly withdrawn with a syringe under a flow of hydrogen at timed intervals by venting the Parr reactor. Constant temperature was maintained using a constant-temperature water bath. Samples were added to $CHCl_3$ in air to destroy the catalyst and terminate the reaction. Concentrations of 1-phenylethanol and acetophenone were determined by gas chromatography with a Chrompack capillary column (Chirasil-Dex CB 25 m × 0.25 mm) and H_2 as carrier gas at a column pressure of 5 psi, an oven temperature of 130 °C, an injector temperature of 250 °C, and an FID at 275 °C. The retention times were acetophenone 5.0 min, (*R*)-1-phenylethanol 8.5 min, and (*S*)-1-phenylethanol 9.1 min. The NMR spectroscopic data of new ruthenium complexes are reported in Table 1.

Synthesis of 1,6-Bis((2-diphenylphosphino)benzo)-3,3,4,4-tetramethyl-2,5-diaza-1,5-hexadiene {$tmeP_2N_2$}. The mixture of 2,3-diamine-2,3-dimethylbutane (0.210 g, 1.8 mmol) and 2-(diphenylphosphino)benzaldehyde (1.110 g, 3.75 mmol) in EtOH (10 mL) was refluxed under Ar for 24 h to give a light yellow precipitate. The mixture was cooled to 0 °C, then filtered and washed with cold EtOH (20 mL), hexanes (10 mL), and diethyl ether (10 mL) and dried under vacuum to give a pale yellow solid (yield: 0.996 g, 80%). Anal. Calcd for $C_{44}H_{42}N_2P_2$: C, 79.98; H, 6.41; N, 4.24. Found: C, 80.15; H, 6.60; N, 4.11. ^1H NMR ($CDCl_3$): δ 8.88 (d, 2H, C*H*=N, $^4J_{HP}$ = 5.2 Hz), 8.06 (dd, 2H, Ar*H*), 7.50−7.30 (m, Ar*H*, 24H), 6.90 (dd, 2H, Ar*H*), 1.00 (s, 12H, CH_3). ^{13}C NMR: δ 155.0 (d, *C*H=N), 140.3 (d, Ph), 137.4 (d, Ph), 136.4 (d, Ph), 134.3 (d, Ph), 132.8 (s, Ph), 129.8 (s, Ph), 128.9 (s, Ph), 128.7 (s, Ph), 128.6 (s, Ph), 127.2 (s, Ph), 65.6 (s, $C(CH_3)_2$), 22.8 (s, CH_3). $^{31}P\{^1H\}$

(10) Abdur-Rashid, K.; Faatz, M.; Lough, A. J.; Morris, R. H. *J. Am. Chem. Soc.* **2001**, *123*, 7473−7474.

(11) Hirel, C.; Vostrikova, K. E.; Pecaut, J.; Ovcharenko, V. I.; Rey, P. *Chem. Eur. J.* **2001**, *7*, 2007−2014.

(12) Hallman, P. S.; McGarvey, B. R.; Wilkinson, G. *J. Chem. Soc. A* **1968**, 3143−3150.

Table 1. NMR Data for the Ruthenium Hydride Complexes

			^{1}H NMR data (δ)				^{31}P NMR data (δ)
	complex	solvent	hydride	CH_3	CH_2, CH, and NH	Ph	
4A	RuHCl{tmeP$_2$(NH)$_2$}	CD_2Cl_2	−17.54 (t), $^2J_{HP}$ = 22.7 Hz	1.68 (s), 1.60 (s)	3.88 (d), 4.15 (d), $^3J_{HH}$ = 10 Hz; 5.6 (br, NH)	7.65 (br), 7.3−7.0 (m), 6.40 (br)	65.9 (br, s)
		CD_2Cl_2 at 200 K	−17.53 (dd), $^2J_{HP}$ = 22.3, 21.6 Hz	1.24 (s), 1.34 (s), 1.54 (s), 1.72 (s)	3.96 (m, 2H, CH_2), 4.31 (d, 1H, CH_2), 4.63 (m, 1H, CH_2), 5.81 (br, 2H, NH)	8.24−6.18 (m)	68.2 (d) 62.7 (d), $^2J_{pp}$ = 31 Hz
4B	RuHCl{tmeP$_2$(NH)$_2$}	CD_2Cl_2	−18.40 (dd), $^2J_{HP}$ = 21.6, 29.2 Hz	1.37 (s), 1.42 (s), 1.44 (s), 1.62 (s)	4.05 (m), 3.94 (m), 4.97 (t, NH). $^3J_{HH}$ = 9 Hz	8.60 (br), 8.09 (t), $^3J_{HH}$ = 8.5 Hz, 7.34−6.7 (m)	63.2 (d) 57.0 (d), $^2J_{PP}$ = 30.3 Hz
5	RuH{tmeP$_2$NNH}	C_6D_6	−23.85 (dd), $^2J_{HP}$ = 25.5, 47.5 Hz	1.23 (s), 1.15 (s), 1.06 (s), 0.98 (s)	4.22 (m), 3.71 (s), 3.40 (br)	8.20 (br), 7.40−6.63 (m)	66.0 (d) 61.1 (d), $^2J_{PP}$ = 17.7 Hz
6	Ru(H)$_2${tmeP$_2$(NH)$_2$}	C_6D_6	−5.28(t), $^2J_{HP}$ = 17.7 Hz	1.24 (s), 0.69 (s)	4.10 (m), 3.49 (m)	8.43 (br), 7.59−6.81 (m)	77.5 (s)
7	RuHCl{tmeP$_2$N$_2$}	CD_2Cl_2	−17.06 (t), $^2J_{HP}$ = 27.5 Hz	1.66 (s), 1.58 (s)	8.91 (d), $^2J_{HP}$ = 7.3 Hz	7.66−6.98 (m)	59.3 (br, s)
		CD_2Cl_2 at 200 K	−16.90 (dd), $^2J_{HP}$ = 20.5, 30.5 Hz	0.88 (s), 1.24 (s), 1.40 (s), 1.80 (s)	9.06 (d), $^2J_{HP}$ = 6.9 Hz, 8.79 (d), $^2J_{HP}$ = 7.1 Hz	7.86−5.80 (m)	58.4 (d) 56.2 (d), $^2J_{pp}$ = 31 Hz
5 + D$_2$		C_6D_6	−5.15 (t), $^2J_{HP}$ = 18 Hz, −5.29 (t), $^2J_{HP}$ = 18 Hz	1.24 (s), 0.69 (s)	4.08 (m), 3.47 (m)	8.43 (br), 7.59−6.81 (m)	77.78 (s), 77.65 (s), 77.52 (s)

NMR: δ −12.51 (s). IR (Nujol): 1639 (s, C=N). MS for $C_{44}H_{42}N_2P_2$: 660.1 (M^+, 6%), 604.1 (76.1%), 330.1 (38%), 288.1 (100%), 183.0 (40.3%).

Synthesis of 1,6-Bis((2-diphenylphosphino)benzo)-3,3,4,4-tetramethyl-2,5-diazahexane {tmeP$_2$(NH)$_2$}. The tmeP$_2$N$_2$ compound (0.500 g, 0.758 mmol) in ether (10 mL) was added to $LiAlH_4$ (29 mg, 0.76 mmol) in ether (20 mL) under Ar. The mixture was refluxed for 14 h. After the resulting solution was cooled to room temperature, 1 mL of water was added to destroy the excess $LiAlH_4$. An aqueous solution of NaOH (10%, 30 mL) was added. The ether layer was collected. The aqueous layer was extracted with ether (10 mL × 3). The combined ether layer was dried over $MgSO_4$ and filtered, and the solvent was removed by vacuum to give a white solid (yield: 0.440 g, 87%). Anal. Calcd for $C_{44}H_{46}N_2P_2$: C, 79.49; H, 6.99; N, 4.21. Found: C, 79.78; H, 6.60; N, 4.10. ^{1}H NMR (C_6D_6): δ 7.70−6.90 (m, 28H, Ar*H*), 4.02 (d, 4H, C*H*$_2$, $^3J_{HH}$ = 6.3 Hz), 1.37 (brs, 2H, N*H*), 0.91 (s, 12H, C*H*$_3$). ^{13}C NMR: δ 147.0 (d, Ph), 137.9 (d, Ph), 135.9 (d, Ph), 134.2 (d, Ph), 133.8 (s, Ph), 129.6 (d, Ph), 129.2 (s, Ph), 128.8 (s, Ph), 128.7 (s, Ph), 127.1 (s, Ph), 59.2 (s, *C*(CH$_3$)$_2$), 45.9 (d, NH*C*H$_2$), 20.9 (s, *C*H$_3$). ^{31}P{^{1}H} NMR: δ −15.86 (s). IR (Nujol): 3177 (w, NH). MS for $C_{44}H_{46}N_2P_2$: 663.3 (M^+ − H, 7%), 332.1 (100%), 275.1 (44%).

Synthesis of RuHCl{tmeP$_2$(NH)$_2$} (4A, 4B). A mixture of tmeP$_2$(NH)$_2$ (140 mg, 0.21 mmol) and $RuHCl(PPh_3)_3$ (192 mg, 0.21 mmol) in THF (5 mL) was refluxed under Ar for 1 h to give a red solution and pink precipitate. Two-thirds of the solvent was removed by vacuum. The mixture was filtered. The solid was washed with ether (1 mL × 3) and dried under vacuum to give a pink powder (121 mg, 73%). The pink powder is composed of two isomers, **4A** and **4B**. The yellow isomer **4A** was isolated in 39% yield by washing the mixture with THF to remove the red isomer **4B**. Isomer **4A**, when heated in CH_2Cl_2 for 16 h, converted into isomer **4B** completely. A yellow crystal of isomer **4A** was obtained by the vapor diffusion of ether into a CH_2Cl_2 solution of **4A** under Ar. Anal. Calcd for $C_{44}H_{47}ClN_2P_2Ru$: C, 65.87; H, 5.90; N, 3.49. Found: C, 65.62; H, 6.02; N, 3.38. IR (Nujol): 3247 (w, NH), 3203 (w, NH), 2007 (m, RuH). MS for $C_{44}H_{47}N_2P_2ClRu$: 802 (M^+, 5.9%), 764 (100%). NMR data: see Table 1.

Synthesis of RuH{tmeP$_2$NNH} (5). A mixture of RuHCl{tmeP$_2$(NH)$_2$} (80 mg, 0.10 mmol) and KO^{t}Bu (17 mg, 0.15 mmol) in toluene (3 mL) was stirred under Ar for 1 h to give a dark red solution. The mixture was filtered through Celite. The solvent was removed by vacuum to give a red residue (yield: 63 mg, 79%). A red crystal of **5** was obtained by the vapor diffusion of hexane into a THF solution of **5** under Ar after a week. IR (Nujol): 3233 (w, NH), 2015 (m, RuH). Anal. Calcd for $C_{48}H_{54}N_2OP_2Ru$ (5·THF): C, 68.80; H, 6.50; N, 3.34. Found: C, 68.36; H, 6.98; N, 3.11. NMR data: see Table 1.

Synthesis of *trans*-RuH$_2${tmeP$_2$(NH)$_2$} (6). Method a. A mixture of RuHCl{tmeP$_2$(NH)$_2$} (20 mg, 0.025 mmol) and KO^{t}Bu (15 mg, 0.13 mmol) in C_6D_6 was sealed in an NMR tube under H_2 (1 atm). A yellow-brown solution was produced after 1 h. The dihydride is not stable under Ar. The brown crystal of **6** was obtained by the vapor diffusion of hexane into the C_6D_6 solution of **6** under H_2. **Method b**. A dark red solution of RuH{tmeP$_2$NNH} (20 mg, 0.025 mmol) in C_6D_6 (0.6 mL) was reacted with 1 atm H_2 to give the yellow dihydride **6**. NMR data: see Table 1.

Synthesis of RuHCl{tmeP$_2$N$_2$} (7). A solution of tmeP$_2$N$_2$ (188 mg, 0.21 mmol) and $RuHCl(PPh_3)_3$ (143 mg, 0.21 mmol) in THF (3 mL) was refluxed under Ar for 1 h to give a red solution and red precipitate. Two-thirds of the solvent was removed by vacuum. The mixture was filtered, and the solid was washed with THF and ether and dried under vacuum to give a pink powder (yield: 126 mg, 75%). A red crystal of **7** was obtained by the vapor diffusion of ether into the CH_2Cl_2 solution of **7** under Ar. Anal. Calcd for $C_{44}H_{43}ClN_2P_2Ru$: C, 66.20; H, 5.43; Cl, 4.44; N, 3.51. Found: C, 66.10; H, 5.22; N, 3.60. NMR data: see Table 1.

Reaction of RuHCl{tmeP$_2$N$_2$} (7) with Base and H$_2$. A mixture of RuHCl{tmeP$_2$N$_2$} (**7**) (20 mg, 0.025 mmol) and KO^{t}Bu (10 mg, 0.10 mmol) in C_6D_6 were sealed in an NMR tube under H_2 (1 atm). The mixture turned green in 10 min and then yellow, to give a solution of the dihydride **6** in 1 h. ^{1}H NMR(C_6D_6) hydrides: δ −5.27 (t, ^2J(HP) = 18.3 Hz). ^{31}P NMR: δ 77.6 (s).

Reaction of [RuH{tmeP$_2$(N)(NH)}] (5) with D$_2$. A solution of RuH{tmeP$_2$NNH} (**5**) (20 mg, 0.024 mmol) in C_6D_6 was reacted with 1 atm of D_2. The dark red solution turned dark brown in 20 min and then dark red in 1 h.

X-ray Diffraction Structure Determination of RuHCl{tmeP$_2$(NH)$_2$} (4A), RuH{tmeP$_2$(N)(NH)} (5), RuH$_2${tmeP$_2$(NH)$_2$} (6), and RuHCl{tmeP$_2$N$_2$} (7). Crystals suitable for X-ray diffraction were obtained by vapor diffusion. Data were collected on a Nonius Kappa-CCD diffractometer using Mo Kα radiation (λ = 0.71073 Å). The CCD data were integrated and scaled using the DENZO-SMN software package, and the structure was solved and refined using SHELXTL V6.0. The crystallographic data are listed in Table 2, and selected bond distances and angles in Tables 3−6. The hydrides were located and refined with isotropic thermal parameters (Figures 1−4).

Table 2. Crystallographic Data for RuHCl{tmeP$_2$(NH)$_2$} (4A), RuH{tmeP$_2$NNH} (5), RuH$_2$\{tmeP$_2$(NH)$_2$\} (6), and RuHCl{tmeP$_2$N$_2$} (7)

	4A($^1/_2$CH$_2$Cl$_2$, $^1/_2$THF)	**5**(THF)	**6**	**7**
formula	$C_{46.50}H_{52}Cl_2N_2O_{0.50}P_2Ru$	$C_{48}H_{54}N_2OP_2Ru$	$C_{44}H_{48}N_2P_2Ru$	$C_{44}H_{43}ClN_2P_2Ru$
fw	880.81	837.94	767.85	798.26
space group	$P\bar{1}$	$P2(1)/n$	$P\bar{1}$	$P2(1)/c$
T, K	150 (1)	150 (1)	150 (1)	150 (1)
A, Å	11.1340(3)	9.3224 (1)	11.2950(2)	11.3980(5)
B, Å	11.2830(3)	12.9914 (1)	12.0470(2)	9.0700(2)
C, Å	18.6220(5)	33.9421(4)	14.9080(2)	35.610(1)
α, deg	80.504(2)	90	75.7729(8)	90
β, deg	75.354(2)	94.899(6)	80.7890(8)	94.718(1)
γ, deg	82.767(2)	90	75.8090(6)	90
V, Å^3	2223.6(1)	4095.74(7)	1895.53(5)	3668.9(2)
Z	2	4	2	4
wavelength, Å	0.71073	0.71073	0.71073	0.71073
ρ_{calc}, mg/m^3	1.316	1.359	1.345	1.445
R_1 (all data)	0.0519	0.0743	0.0549	0.0990
wR_2	0.1176	0.0844	0.0912	0.1172

Table 3. Selected Bond Distances and Angles for RuHCl{tmeP$_2$(NH)$_2$} (4A)

Distances, Å			
Ru(1)−H(1RU)	1.56(3)	Ru(1)−N(1)	2.179(2)
Ru(1)−N(2)	2.189(2)	Ru(1)−P(1)	2.2519(6)
Ru(1)−P(2)	2.2348(7)	Ru(1)−Cl(1)	2.5970(6)
N(1)−C(17)	1.487(3)	N(1)−C(1)	1.521(3)
N(1)−H(1A)	0.93	N(2)−C(47)	1.485(3)
N(2)−C(2)	1.532(3)	N(2)−H(2A)	0.93

Angles, deg			
H(1RU)−Ru(1)−N(1)	85(1)	H(1RU)−Ru(1)−N(2)	87(1)
N(1)−Ru(1)−N(2)	79.59(8)	H(1RU)−Ru(1)−P(2)	90(1)
N(1)−Ru(1)−P(2)	166.81(6)	N(2)−Ru(1)−P(2)	87.86(6)
H(1RU)−Ru(1)−P(1)	86(1)	N(1)−Ru(1)−P(1)	91.13(6)
N(2)−Ru(1)−P(1)	168.37(6)	P(2)−Ru(1)−P(1)	100.81(2)
H(1RU)−Ru(1)−Cl(1)	179(1)	N(1)−Ru(1)−Cl(1)	93.66(5)
N(2)−Ru(1)−Cl(1)	93.92(6)	P(2)−Ru(1)−Cl(1)	91.20(2)
P(1)−Ru(1)−Cl(1)	93.64(2)		

Table 4. Selected Bond Distances and Angles for RuH{tmeP$_2$NNH} (5)

Distances, Å			
Ru(1)−H(1RU)	1.54(3)	Ru(1)−N(1)	2.164(2)
Ru(1)−N(2)	2.001(2)	Ru(1)−P(1)	2.2495(7)
Ru(1)−P(2)	2.2303(7)		
N(1)−C(7)	1.488(3)	N(1)−C(1)	1.513(3)
N(2)−C(2)	1.482(3)	N(2)−C(8)	1.475(3)

Angles, deg			
H(1RU)−Ru(1)−N(1)	90.5(9)	H(1RU)−Ru(1)−N(2)	116.9(9)
N(1)−Ru(1)−N(2)	80.04(8)	H(1RU)−Ru(1)−P(2)	91.6(9)
N(1)−Ru(1)−P(2)	170.44(6)	N(2)−Ru(1)−P(2)	90.68(6)
H(1RU)−Ru(1)−P(1)	76.5(9)	N(1)−Ru(1)−P(1)	91.74(6)
N(2)−Ru(1)−P(1)	164.04(6)	P(2)−Ru(1)−P(1)	97.82(2)

Table 5. Selected Bond Distances and Angles for Ru(H)$_2$\{tmeP$_2$(NH)$_2$\} (6)

Distances, Å			
Ru(1)−H(1RU)	1.59(3)	Ru(1)−H(2RU)	1.62(3)
Ru(1)−N(2)	2.196(2)	Ru(1)−N(1)	2.182(2)
Ru(1)−P(2)	2.2265(6)	Ru(1)−P(1)	2.2205(6)
N(1)−C(7)	1.490(3)	N(2)−H(2N)	0.88(3)
N(1)−H(1N)	0.88(3)	N(1)−C(1)	1.517(3)
N(2)−C(2)	1.522(3)	N(2)−C(8)	1.492(3)

Angles, deg			
H(1RU)−Ru(1)−H(2RU)	175(1)		
H(1RU)−Ru(1)−N(1)	85(1)	H(1RU)−Ru(1)−N(2)	90(1)
H(1RU)−Ru(1)−P(1)	87(1)	H(1RU)−Ru(1)−P(2)	93(1)
H(2RU)−Ru(1)−N(2)	86.3(9)	H(2RU)−Ru(1)−P(2)	89.5(9)
H(2RU)−Ru(1)−P(1)	95.7(9)	H(2RU)−Ru(1)−N(1)	91.2(9)
N(1)−Ru(1)−P(2)	169.75(5)	N(2)−Ru(1)−P(2)	91.17(5)
N(2)−Ru(1)−P(1)	170.77(5)	N(1)−Ru(1)−P(1)	92.25(5)
N(1)−Ru(1)−N(2)	78.67(7)	P(2)−Ru(1)−P(1)	97.85(2)

Results and Discussion

Synthesis of the Ligands {tmeP$_2$N$_2$} and {tmeP$_2$(NH)$_2$}. The new tetradentate ligand {tmeP$_2$N$_2$} is easily prepared[13] in 80% yield by the condensation reaction of $NH_2CMe_2CMe_2NH_2$ with 2 equiv of $PPh_2(C_6H_4$-2-CHO) (eq 1). The spectroscopic properties are very similar to those of MeP$_2$N$_2$.[4] The presence of the imine groups is signaled by a C=N stretch at 1639 cm^{-1} in the IR spectrum, a doublet ($^4J_{PH}$ = 5.2 Hz) at 8.88 ppm in the ^{1}H NMR spectrum, and a doublet ($^3J_{PC}$ = 23.0 Hz) at 155.0 ppm in the ^{13}C{^{1}H} NMR spectrum. The diamine, {tmeP$_2$(NH)$_2$}, is obtained by the reduction of {tmeP$_2$N$_2$} with LiAlH$_4$ in 87% yield (eq 2). The NH protons appear at 1.37 ppm in the ^{1}H NMR. NaBH$_4$ is

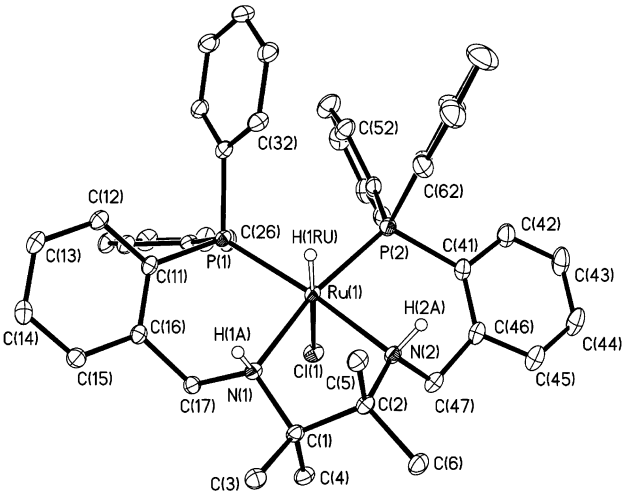

Figure 1. Molecular structure of RuHCl{tmeP$_2$(NH)$_2$} (**4A**).

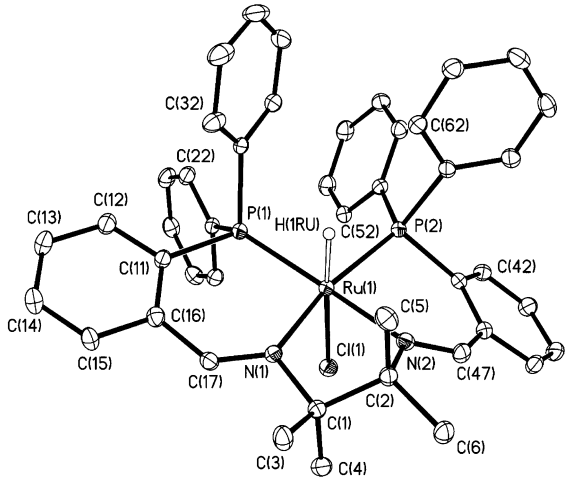

Figure 2. Molecular structure of RuHCl{tmeP$_2$N$_2$} (**7**).

Table 6. Selected Bond Distances and Angles for RuHCl{tmeP$_2$N$_2$} (7)

Distances, Å			
Ru(1)−H(1RU)	1.62(4)	Ru(1)−N(1)	2.099(3)
Ru(1)−N(2)	2.112(3)	Ru(1)−P(1)	2.255(1)
Ru(1)−P(2)	2.263(1)	Ru(1)−Cl(1)	2.591(1)
N(1)−C(17)	1.286(5)	N(1)−C(1)	1.537(5)
N(2)−C(2)	1.516(4)	N(2)−C(47)	1.278(5)

Angles, deg			
H(1RU)−Ru(1)−N(1)	89(1)	H(1RU)−Ru(1)−N(2)	90(1)
N(1)−Ru(1)−N(2)	79.1(1)	H(1RU)−Ru(1)−P(2)	88(1)
N(1)−Ru(1)−P(2)	166.86(9)	N(2)−Ru(1)−P(2)	88.01(8)
H(1RU)−Ru(1)−P(1)	82(1)	N(1)−Ru(1)−P(1)	94.00(9)
N(2)−Ru(1)−P(1)	169.61(8)	P(2)−Ru(1)−P(1)	98.32(4)
H(1RU)−Ru(1)−Cl(1)	177(1)	N(1)−Ru(1)−Cl(1)	91.78(8)
N(2)−Ru(1)−Cl(1)	87.29(8)	P(2)−Ru(1)−Cl(1)	90.38(3)
P(1)−Ru(1)−Cl(1)	100.83(3)		

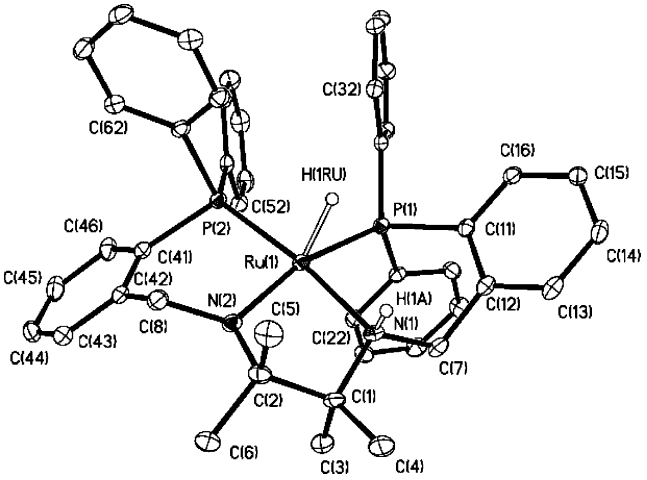

Figure 3. Molecular structure of the hydridoamido complex **5**.

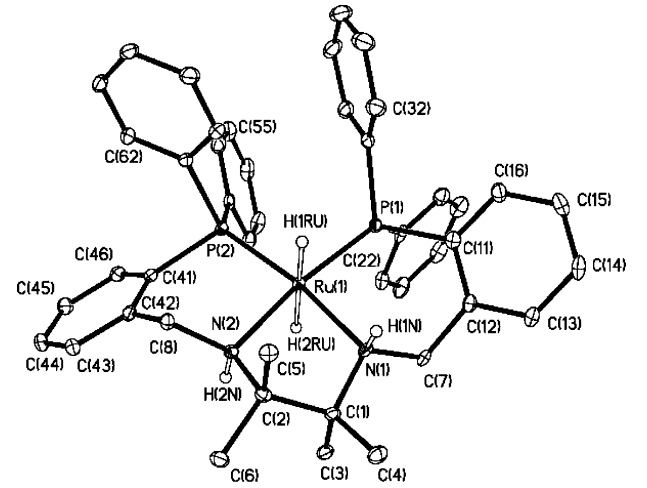

Figure 4. Molecular structure of the dihydridoamine complex **6**.

not suitable forthis reduction. Its use led to a mixture of incompletely reduced compounds.

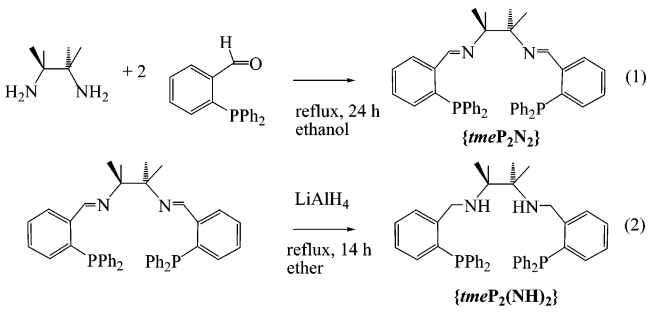

Synthesis, Isomerization Reactions, and Structures of RuHCl{tmeP$_2$(NH)$_2$} 4A and 4B. The pink complex *trans*-RuHCl{tmeP$_2$(NH)$_2$} is prepared as a mixture of isomers **4A** and **4B** in 73% yield by the reaction of RuHCl(PPh$_3$)$_3$ with 1 equiv of the ligand {tmeP$_2$(NH)$_2$} in refluxing THF (eq 3). The mixture is

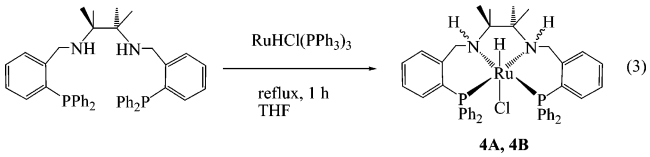

stable in the solid state for days under air, but it is air sensitive in solution. The isomers are present in variable amounts. The yellow isomer **4A** is only slightly soluble in THF and can be isolated by washing the pink solid mixture with THF to remove the red isomer **4B**. Isomer **4A** can be fully converted to isomer **4B** by heating the CH_2Cl_2 solution of **4A** under Ar overnight (eq 4). This shows that isomer **4B** is the thermodynamically favored product and isomer **4A** is the kinetically favored product. This also explains why the ratio of the two isomers in the synthesis of the complex depends on the concentration, temperature, and the reaction time.

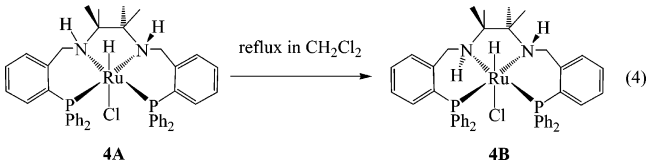

The structure of **4A** was established by the X-ray diffraction study that revealed the octahedral configuration shown in Figure 1. The hydride and chloride ligands are *trans* to each other. Isomer **4A** has two NH hydrogen atoms *syn* to the hydride ligand, with H(1A) axial and H(2A) equatorial with respect to the RuNCCN five-membered ring. The stereogenic nitrogen atoms have opposite configurations (*R* and *S*). At 200 K, **4A** exhibits two doublets at 68.2 and 62.7 ppm in the ^{31}P-{^{1}H} NMR spectrum and four singlets for the methyl groups and a doublet of doublets for the hydride at −17.5 ppm in the ^{1}H NMR spectrum. At room temperature the spectra simplify to a broad peak at 65.9 ppm for the ^{31}P{^{1}H} NMR and two singlets for the methyls and a triplet for the hydride for the ^{1}H NMR. A rapid flipping of the RuNHCMe$_2$CMe$_2$NH five-membered ring[14] at room temperature would interchange axial and equatorial NH and methyl groups and interchange the environments of the PPh$_2$ groups, thus averaging their chemical shifts. Therefore this tetradentate ligand, despite its hindered appearance, is quite flexible.

Isomer **4B** exhibits two doublets in the ^{31}P NMR spectrum and four singlets for the methyl groups and a doublet of doublets for the hydride in the ^{1}H NMR. The two phosphorus atoms and NH groups are not equivalent because there is no molecular symmetry even with a flipping of the backbone. The structure of **4B** likely has one NH hydrogen *syn* to the chloride and the other NH *syn* to the hydride, both in axial positions with respect to the RuNCCN ring, as shown in eq 4. Two related X-ray crystal structures of RuCl$_2$(enP$_2$(NH)$_2$) and RuCl$_2$(cyP$_2$(NH)$_2$) were reported by Gao et al.[1] The NH groups in these complexes are on opposite sides of the tetradentate ligand plane as proposed for isomer **4B**. A small amount of a third isomer could be observed after heating isomer **4B** overnight in THF. The third isomer was not isolated. The structure of the third isomer is proposed to have two NH hydrogen atoms *syn* to chloride.

Synthesis and Structure of the Diimine Complex RuHCl{tmeP$_2$N$_2$} (7). The complex *trans*-RuHCl-

(13) Jeffery, J. C.; Rauchfuss, T. B.; Tucker, P. A. *Inorg. Chem.* **1980**, *19*, 3306−3316.
(14) Abdur-Rashid, K.; Clapham, S. E.; Hadzovic, A.; Harvey, J. N.; Lough, A. J.; Morris, R. H. *J. Am. Chem. Soc.* **2002**, *124*, 15104−15118.

{tmeP$_2$N$_2$} (**7**) is prepared in 75% yield as a sparingly soluble pink powder by heating a solution of RuHCl(PPh$_3$)$_3$ in THF with the ligand {tmeP$_2$N$_2$} (eq 5). In the preparation of **7**, only one isomer is formed. Therefore, the occurrence of isomers **4A** and **4B** must be related to the direction of the NH groups.

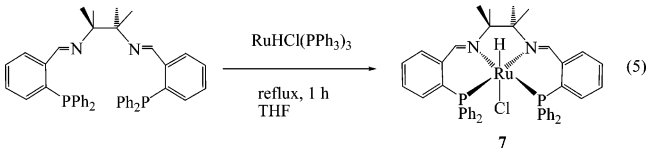

(5)

7

The X-ray crystal structure of **7** shows a *trans* octahedral complex (Figure 2). The bond distances of C(47)−N(2) and C(17)−N(1) are 1.278(5) and 1.286(5) Å, as expected for imine groups. The Ru−P bond lengths of **7** (2.255(1) and 2.263(1) Å) are almost identical to those of **4A** (2.252(1) and 2.235(1) Å, while the Ru−N bond lengths are shorter (2.099(3) and 2.112(3) vs 2.179(2) and 2.189(2) Å, respectively). Those of **7** are similar to the bond lengths in RuCl$_2$(cyP$_2$N$_2$), with Ru−P bond lengths of 2.288(2) and 2.295(2) Å and Ru−N bond lengths of 2.091(5) and 2.100(5) Å.[1]

Evidence for the proposed structure is also provided by the ^{1}H NMR spectrum that reveals a triplet for the hydride resonance at −17.1 ppm and a doublet for the imine groups at 9.1 ppm. The triplet pattern of the hydride and doublet of the imine hydrogen atoms are due to coupling to the phosphorus nuclei. The ^{31}P NMR spectrum has a broad peak at 59 ppm. At 200 K, the ^{31}P{^{1}H} NMR spectrum of **7** in CD_2Cl_2 exhibits two doublets at 58.4 and 56.2 ppm, while the ^{1}H NMR spectrum shows four singlets for the methyl groups, a doublet of doublets for the hydride at −16.9 ppm, and two doublets for the imine hydrogen atoms. These data are similar to the spectroscopic properties of *trans*-RuHCl{tmeP$_2$(NH)$_2$} (**4A**), again providing evidence for the flipping of the RuNCMe$_2$CMe$_2$N ring. The similarity of the NMR spectra and crystal structures of **4A** and **7** suggests that the sp^2- and sp^3-hybridized nitrogen donors place the Ru in a similar electronic state.

Synthesis and Structure of the Hydridoamido Complex RuH{tmeP$_2$NNH} (5). The reaction of a mixture of **4A** and **4B** with KO^{t}Bu under Ar in THF produces the red amido complex RuH{tmeP$_2$NNH} (**5**) in 79% yield (eq 6). This complex is air sensitive in both the solid state and in solution.

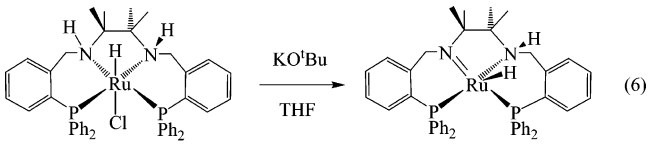

(6)

4A **5**

Complex **5** was crystallized under Ar, and the structure was determined by X-ray diffraction (Figure 3). The amido complex **5** is best viewed as a distorted trigonal bipyramidal with the N(1) and P(2) in pseudoaxial positions, forming the angle N(1)−Ru(1)−P(2) = 170.44(6)°. This places the amido nitrogen in an equatorial position for favorable dative π-bonding to Ru. This interaction causes the hydride and P(1) to squeeze together with H(1RU)−Ru(1)−P(1) = 76.5(9)°. This is a geometry very similar to that of the only other structurally characterized hydridoamido complex, RuH(NHCMe$_2$CMe$_2$NH$_2$)(PPh$_3$)$_2$.[14] The amido nitrogen−ruthenium bond length of 2.001(2) Å (Ru(1)−N(2)) is similar to the ruthenium−nitrogen double bond distance of 1.967(1) Å for the latter complex and shorter than the amine nitrogen−ruthenium distance, which is 2.164(2) Å (Ru(1)−N(1)). The N−H bond is in an axial position with respect to the RuNCCN ring and is aligned with the Ru−H bond. The doublet of doublets pattern for the hydride at −23.8 ppm in the ^{1}H NMR spectrum and two doublets at 66.0 and 61.1 ppm with $^2J_{PP}$ = 17.7 Hz in the ^{31}P NMR spectrum signal the presence of the two nonequivalent phosphorus atoms, as observed in the X-ray structure. Even though the P−Ru−P angles are similar (98−101°) in complexes **5**, **4**, and **7**, the coupling constant $^2J_{PP}$ of the amido complex **5** is noticeably smaller than those of the octahedral complexes **4** and **7** (approximately 31 Hz). No change was observed in the ^{1}H and ^{31}P{^{1}H} NMR spectra of **5** in toluene-d_8 at 200 K.

Synthesis and Structure of the Dihydridoamine Complex RuH$_2${tmeP$_2$(NH)$_2$} (6). The amido complex RuH{tmeP$_2$NNH} reacts with dihydrogen to produce exclusively the dihydride complex *trans*-RuH$_2${tmeP$_2$(NH)$_2$}, **6** (eq 7). This complex is only stable under H$_2$. It loses H$_2$ under Ar in solution and the solid state to give complex **5**. This complex can also be prepared directly in about 40% yield from complex **4** by reaction with KO^{t}Bu under H$_2$ (1 atm) in C_6D_6, but other hydride-containing species are also produced.

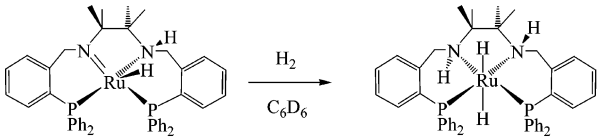

(7)

5 **6**

Complex **6** was crystallized under H$_2$, and the structure was determined by X-ray diffraction (Figure 4). Complex **6** has an octahedral geometry with approximately C_2 symmetry. The Ru(1)−N(1) and Ru(1)−N(2) bond lengths of 2.196(2) and 2.182(2) Å are comparable to those of RuH$_2$(tmen)(R-binap), 2.202(2) and 2.193(2) Å.[10] The two hydrides are *trans* (H(1Ru)−Ru(1)−H(2Ru) 175(1)°). Each of the two N−H bonds is aligned with one of the two Ru−H bonds. The X-ray crystal structure also reveals that the RuH···H$_{ax}$N distances of about 2.4 Å are at the outer limit of hydridic-protonic bonding.[15,16] The C_2 symmetry of the complex in solution is revealed by the triplet pattern at −5.28 ppm ($^2J_{PH}$ = 18 Hz) of the hydride in the ^{1}H NMR spectrum and a sharp singlet at 77.5 ppm in the ^{31}P{^{1}H} NMR spectrum. The dihydride *trans*-RuH$_2$(tmen)(R-binap) shows similar features, notably a hydride triplet at −4.8 ppm with a small coupling of 17 Hz.[10]

The stereochemistry of **6** also can be established by reacting RuH{tmeP$_2$NNH} with D$_2$(g) to form the *trans* isotopomer RuHD{tmeP$_2$(ND)(NH)} (shown in eq 8) along with other isotopomers resulting from further H/D exchange at RuH, NH, and CH$_2$. The isotopomers with

(15) Lough, A. J.; Park, S.; Ramachandran, R.; Morris, R. H. *J. Am. Chem. Soc.* **1994**, *116*, 8356−8357.
(16) Crabtree, R. H.; Siegbahn, P. E. M.; Eisenstein, O.; Rheingold, A. L.; Koetzle, T. F. *Acc. Chem. Res.* **1996**, *29*, 348−354.

Scheme 2. Mechanism for H/D Exchange between D_2 (g) and Complex 6-d_2[a]

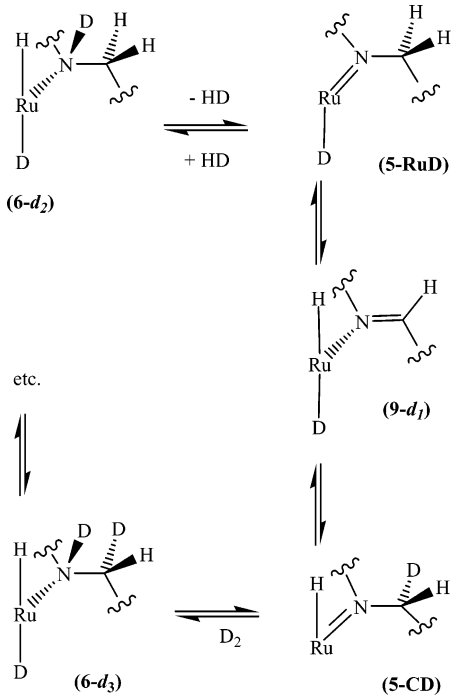

[a] Only atoms directly involved are shown for clarity.

a *trans* H−Ru−D motif produce overlapping triplets for the hydrides in the ^{1}H NMR spectrum at −5.15 ppm. This large downfield shift of 0.13 ppm from the hydride resonance of undeuterated **6** is caused by the large *trans* influence of deuterium. This proves that the hydrides are *trans* in the dihydride since a deuterium *cis* to a hydride would not have such a large influence on the chemical shift.

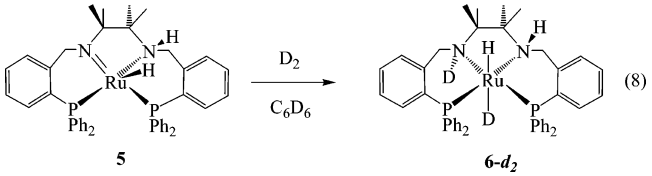

(8)

The three overlapped singlets at 77.78, 77.65, and 77.52 ppm in the ^{31}P{^{1}H} NMR spectrum suggest that there are at least three different isotopomers in the exchange process. Surprisingly, the analysis by ^{1}H NMR shows the slow decrease of the peaks due to CH_2 groups caused by a hydrogen−deuterium exchange process. The exchange of methylene protons with solvent deuteriums was reported in a ruthenium(II) hydrido complex of 2,6-(diphenylphosphinomethyl)pyridine.[17] We propose that the C−D bonds form by a β-hydride elimination (Scheme 2) from the amido complex **5** and its isotopomers to produce imine complexes of the type **9-d_1**.[6] This step might proceed via an intermediate where the imine C=N is π-bonded to ruthenium. The addition of the deuteride to the imine creates a new C−D bond. In the presence of extra D_2, this process eventually leads to almost complete deuteration of the methylene positions. There is no deuteration of the phenyl C−H bonds.

Hydrogenation of Acetophenone Catalyzed by Complex 5. Complex **5** in benzene, toluene, or 2-propanol is a well-defined catalyst for the hydrogenation of acetophenone. Some rate determination measurements have served to define the kinetic properties (Table 7).[9,10,14]

In benzene solution, complex **5** is 24 times less active than RuH_2(tmen)(R-binap) and 141 times less active than the analogous catalyst system RuHCl(cyP_2($NH)_2$)/KO^{t}Bu (entries 1, 2, and 3 in Table 7). It is significant that replacing a cyclohexyl backbone between the amines in the last complex with a tetramethylethylene backbone in **5** results in such a reduction in rate. Presumably this is a combination of steric and electronic interference of the addition of dihydrogen to the amido complex, the rate-determining step of the catalytic reaction, at least for the catalyst system **1**/KO^{t}Bu/^{i}PrOH. Complex **5** is 4 times more active in 2-propanol than in benzene (entry 4) and does not require the addition of base for activity. The increase in activity of this catalyst as well as that of **4A/4B**/KO^{t}Bu (entry 5) and that of **1**/KO^{t}Bu (entry 6) in 2-propanol compared to similar systems in benzene can be attributed to the more polar solvent stabilizing the transition state of what is believed to be the turnover limiting step, the heterolytic splitting of dihydrogen. Complex **5** in ^{i}PrOH shows activity similar to that of the catalyst system **4A/4B**/KO^{t}Bu/^{i}PrOH, where a mixture of the isomers of the precatalyst is used. Therefore the isomers of **4** react with base quickly to form the amido complex **5**, which then serves as the catalyst in the hydrogenation of acetophenone (as shown in Scheme 1 for precatalyst **1**). This also indicates that potassium ions do not play a role in accelerating the catalysis for this system in 2-propanol, although such an effect has been reported for a $RuCl_2$(binap)(dpen) system.[18] No significant potassium effect was observed in the use of complex **1** either.[9] However the tmeP_2($NH)_2$ systems (entries 4 and 5) are more than 1000 times less active than the corresponding catalyst system **1**/KO^{t}Bu/^{i}PrOH (entry 6).

Hydrogenation of Acetophenone Catalyzed by Complex 7 and Base. RuHCl{tmeP_2N_2} reacts with KO^{t}Bu in 2-propanol under H_2 (6 atm) to produce a catalytic system for the hydrogenation of acetophenone. The initial rate of hydrogenation catalyzed by this system (entry 7) is listed relative to the other catalysts in Table 7.[9]

For comparison the diimine complex RuHCl{(R,R)-cyP_2N_2} (**8**) was prepared by a method similar to that for complex **7**. This complex was found to produce a catalyst that is 50 times more active than the RuHCl{tmeP_2N_2} precatalyst (entry 8 vs entry 7 in Table 7) and gives *R*-1-phenylethanol with an ee of ca. 37%. The diamine system is also more active than the diimine system under these conditions (entries 6 vs 8). However, the reason the RuHCl{tmeP_2N_2}/base system is about 3 times more active than the amidoamine complex (entries 4 and 5 in Table 7) is not clear at this stage.

Reaction of RuHCl{tmeP_2N_2} (7) with Base and H_2. The diimine precatalyst *trans*-RuHCl{tmeP_2N_2} can be converted to the diaminedihydride catalyst *trans*-Ru(H)$_2${tmeP_2($NH)_2$} given a sufficiently long reaction time

(17) Rahmouni, N.; Osborn, J. A.; De Cian, A.; Fischer, J.; Ezzamarty, A. *Organometallics* **1998**, *17*, 2470−2476.

(18) Hartmann, R.; Chen, P. *Angew. Chem., Int. Ed.* **2001**, *40*, 3581−3585.

Table 7. Comparison of Initial Rates of Reaction of Catalyst Systems for the Hydrogenation of Acetophenone (0.167 M) under 6 atm H_2 at 293 K

entry	catalyst	solvent	[Ru]	rate (M s^{-1})	rate/[Ru]	relative rates	ref
1	**5**	C_6H_6	2.0×10^{-4}	9×10^{-7}	4.5×10^{-3}	1	this work
2	RuH_2(tmen)(*R*-binap)	C_6H_6	2.3×10^{-4}	3×10^{-5}	0.12	24	14
3	**1**/KO^{t}Bu	C_6H_6	2.0×10^{-4}	1.2×10^{-4}	0.60	141	9
4	**5**	^{i}PrOH	2.0×10^{-4}	3.7×10^{-6}	0.02	4	this work
5	**4A/4B**/KO^{t}Bu	^{i}PrOH	2.0×10^{-4}	4.6×10^{-6}	0.02	4	this work
6	**1**/KO^{t}Bu	^{i}PrOH	2.0×10^{-4}	5.0×10^{-3}	25	5555	9
7	**7**/KO^{t}Bu	^{i}PrOH	2.0×10^{-4}	1.3×10^{-5}	0.065	14	this work
8	**8**[a]/KO^{t}Bu	^{i}PrOH	2.0×10^{-4}	6.0×10^{-4}	3	667	this work

[a] RuHCl{(R,R)-cyP_2N_2}.

Scheme 3. Catalytic Cycle Showing the Structures of the Catalytic Species

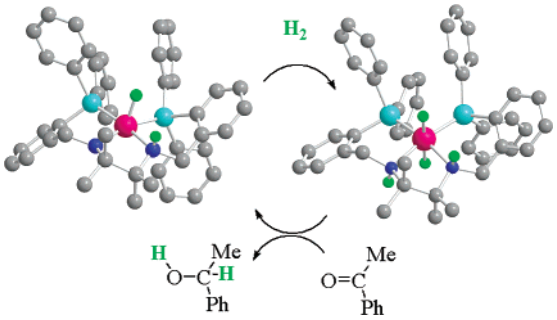

or higher temperatures (eq 9). The mechanism must involve β-hydride addition as in Scheme 2. Therefore the imine functions of the ligand are hydrogenated to the amine functions in the course of the reaction. A similar diimine dichloride complex has been reduced to the corresponding diamine dichloride complex by use of $NaBH_4$.[6]

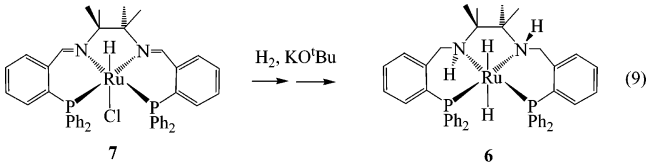

Proposed Mechanism for the Hydrogenation of Acetophenone. The structural studies and experimental observations of these complexes derived from the {tmeP_2(N$H)_2$} ligand provide evidence for the mechanism of hydrogenation proposed earlier for the related {cyP_2(N$H)_2$} system (Scheme 1). Specifically the two catalytic species, the *trans*-dihydride **6** and the hydridoamido complex **5**, have been completely characterized and react in a catalytic fashion as shown in Scheme 3. For the {cyP_2(N$H)_2$} system the dihydride was observed only in solution and the amido complex was too unstable to be characterized. The hydridoamido complex **5** is proposed to coordinate dihydrogen and split it heterolytically[19,20] into a hydride on ruthenium and proton on nitrogen to produce the *trans*-dihydride **6**.[14] As mentioned, the observed increase in the rate of hydrogenation on going from the less polar solvent benzene to the more polar solvent 2-propanol lends support to this proposal. The concerted transfer of hydride and proton to the ketone in the outer coordination sphere[21–23] as shown in Figure 5 results in the ionic hydrogenation[24]

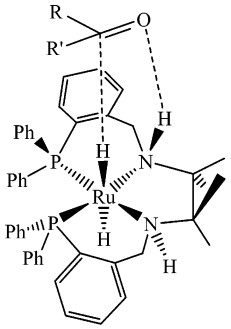

Figure 5. Proposed transition state for the ionic hydrogenation of the ketone in the outersphere of the dihydride complex **6**.

of the ketone and regeneration of the hydridoamido complex.

Conclusions

The new tetradentate ligands $PPh_2C_6H_4CH{=}NCMe_2CMe_2N{=}CHC_6H_4PPh_2$ {tmeP_2N_2} and $PPh_2C_6H_4CH_2NHCMe_2CMe_2NHCH_2C_6H_4PPh_2$ {tmeP_2(N$H)_2$} were prepared and used to make the new complexes RuHCl{tmeP_2(N$H)_2$} (**4**), RuH{tmeP_2NNH} (**5**), *trans*-RuH_2{tmeP_2(N$H)_2$} (**6**), and RuHCl{tmeP_2N_2} (**7**). The structure of **4** as isomer **4A** shows for the first time the presence of two N–H bonds on the same side as the Ru–H bond in such tetradentate ligand complexes. The ease of formation of the isomers derived from the different configurations at nitrogen might explain why the ee of the alcohol product produced by catalysts containing the (S,S)-cyP_2(N$H)_2$ ligand can be high for transfer hydrogenation and low for H_2-hydrogenation.[9] The formation of *cis* and *trans* dihydrides at ruthenium is an alternative explanation that cannot be ruled out at this stage. The Ru hydridoamido complex **5** quickly reacts with H_2 to give the dihydridoamine complex **6** as proposed in the catalytic cycle for the analogous RuH{cyP_2NNH}/RuH_2{cyP_2(N$H)_2$} system. This provides additional evidence for the mechanism of the hydrogenation of ketones catalyzed by these tetradentate ligand systems.[9] Alternative, more classical mechanisms that involve the coordination of the substrate to the metal

(19) Morris, R. H. In *Recent Advances in Hydride Chemistry*; Peruzzini, M., Poli, R., Eds.; Elsevier: Amsterdam, 2001; pp 1–38.
(20) Kubas, G. J. *Metal Dihydrogen and Sigma-Bond Complexes*; Kluwer Academic/Plenum: New York, 2001.
(21) Clapham, S.; Hadzovic, A.; Morris, R. H. *Coord. Chem. Rev.* **2004**, in press.
(22) Noyori, R.; Ohkuma, T. *Angew. Chem., Int. Ed.* **2001**, *40*, 40–73.
(23) Casey, C. P.; Johnson, J. B. *J. Org. Chem.* **2003**, *68*, 1998–2001.
(24) Bullock, R. M. *Chem. Eur. J.* **2004**, *10*, 2366–2374.

can be ruled out because they would have to proceed via decoordination of a donor group of the tetradentate ligand, a very improbable event under the mild conditions of catalysis described here. The correct steric and electronic properties of the ligand are clearly very important for the activation of dihydrogen, and therefore the catalyst activity. The exchange of deuterium for hydrogen on the CH_2 groups in the dihydride complex suggests that the reversible formation of an imine ligand is occurring by β-hydride elimination.

Acknowledgment. This work was supported in part by a discovery grant to R.H.M. from NSERC Canada and a PRF grant, as administered by the American Chemical Society.

Supporting Information Available: X-ray crystallographic file (CIF) containing X-ray structural information for complexes **4A**, **5**, **6**, and **7**. This material is available free of charge via the Internet at http://pubs.acs.org.

OM049565K